Modeling and characterization of dielectrophoretically structured piezoelectric composites using piezoceramic particle inclusions with high aspect ratios

D. A. van den Ende, R. A. Maier, P. L. M. J. van Neer, S. van der Zwaag, C. A. Randall et al.

Related Articles

Enhanced piezoelectric and ferroelectric properties in the BaZrO3 substituted BiFeO3-PbTiO3
Appl. Phys. Lett. 102, 022905 (2013)

Structural diversity of the (Na1−xKx)0.5Bi0.5TiO3 perovskite at the morphotropic phase boundary
J. Appl. Phys. 113, 024106 (2013)

First-principles based multiscale model of piezoelectric nanowires with surface effects
J. Appl. Phys. 113, 014309 (2013)

Large decrease of characteristic frequency of dielectric relaxation associated with domain-wall motion in Sb5+-modified (K,Na)NbO3-based ceramics
Appl. Phys. Lett. 101, 252905 (2012)

Enhanced piezoelectric performance from carbon fluoropolymer nanocomposites
J. Appl. Phys. 112, 124104 (2012)

Additional information on J. Appl. Phys.

Journal Homepage: http://jap.aip.org/
Journal Information: http://jap.aip.org/about/about_the_journal
Top downloads: http://jap.aip.org/features/most_downloaded
Information for Authors: http://jap.aip.org/authors

Modeling and characterization of dielectrophoretically structured piezoelectric composites using piezoceramic particle inclusions with high aspect ratios

D. A. van den Ende,[1,2,3,a)] R. A. Maier,[4] P. L. M. J. van Neer,[5] S. van der Zwaag,[3] C. A. Randall,[4] and W. A. Groen[1,3]

[1]*Holst Centre-TNO, HTC31, 5605 KN Eindhoven, The Netherlands*
[2]*TNO (Netherlands Organization for Applied Scientific Research), Materials for Integrated Products Department, Rondom 1, 5612 AP Eindhoven, The Netherlands*
[3]*Novel Aerospace Materials Group, Faculty of Aerospace Engineering, Delft University of Technology, Kluyverweg 1, 2629 HS Delft, The Netherlands*
[4]*Materials Research Institute, The Pennsylvania State University, University Park, Pennsylvania 16801, USA*
[5]*TNO, Department of Process and Instrumentation Development, Stieltjesweg 1, 2628 CK Delft, The Netherlands*

In this work, the piezoelectric properties at high electric fields of dielectrophoretically aligned PZT—polymer composites containing high aspect ratio particles (such as short fibers) are presented. Polarization and strain as a function of electric field are evaluated. The properties of the composites are compared to those of PZT-polymer composites with equiaxed particles, continuous PZT fiber-polymer composites, and bulk PZT ceramics. From high-field polarization and strain measurements, the effective field dependent permittivity and piezoelectric charge constant in the poling direction are determined for dielectrophoresis structured PZT-polymer composites, continuous PZT fiber-polymer composites, and bulk PZT ceramics. The changes in dielectric properties of the inclusions and the matrix at high fields influence the dielectric and piezoelectric properties of the composites. It is found that the permittivity and piezoelectric charge constants increase towards a maximum at an applied field of around 2.5-5 kV/mm. The electric field at which the maximum occurs depends on the aspect ratio and degree of alignment of the inclusions. Experimental values of d_{33} at low and high applied fields are compared to a model describing the composites as a continuous polymer matrix containing PZT particles of various aspect ratios arranged into chains. Thickness mode coupling factors were determined from measured impedance data using fitted equivalent circuit model simulations. The relatively high piezoelectric strain constants, voltage constants, and thickness coupling factors indicate that such aligned short fiber composites could be useful as flexible large area transducers. © *2013 American Institute of Physics*. [http://dx.doi.org/10.1063/1.4775815]

INTRODUCTION

Piezoelectric materials are used in many applications as sensing, actuating, or energy harvesting elements. Piezoelectric ceramics possess excellent electromechanical coupling coefficients but suffer from high density, poor mechanical properties, and difficult processing. Piezoelectric ceramic-polymer composites are a class of materials where a piezoelectric ceramic phase is embedded in a polymer matrix. The shape and connectivity pattern of the PZT phase not only determines the aforementioned properties[1] but also the ease of processing. For instance, 1-3 composites can achieve higher coupling coefficients and voltage sensitivity than monolithic ceramics, but are generally difficult to process. This processing obstacle results in relatively costly materials which are less suitable for large scale cost effective manufacturing. Alternatively, low-cost composites such as 0-3 PZT particle-polymer composites are flexible, easy to process,

and can be applied at low temperatures and in large areas.[2] However, while the limited connectivity of the ceramic phase enables flexibility of the composites, it also causes these types of composites to suffer from inferior piezoelectric properties compared to their 1-3 counterparts. The decrease in properties is due to limited connectivity in combination with the mismatch in permittivity between the matrix and the piezoelectric inclusions.[3,4]

Dielectrophoresis (DEP)[5] is a technique which allows *in situ* forming of quasi 1-3 structures from randomly oriented dielectric particles in a thermosetting resin. When an alternating electric field is applied during curing of the matrix, the dielectric particles in the composite coalesce to form chains, oriented in the direction of the applied field.[6,7] Piezoelectric coupling in the direction of alignment increases for composites with alignment of equiaxed particles.[8] Composites with aligned elongated particles, i.e., particles of aspect ratio higher than one, have also been assessed.[9–11] Piezoelectric composites with randomly oriented elongated particles inclusions demonstrate improved transducer properties.[12] Low field piezoelectric constants of DEP aligned short fiber

a)Author to whom correspondence should be addressed. Electronic mail: daan.vandenende@tno.nl.

composites are significantly higher than conventional 0-3 composites. At low volume fractions of PZT, d_{33} values can reach about 100 times the values of conventional 0-3 PZT composites with equiaxed particle inclusions.[11] However, further insight is needed into the high field properties and resonance characteristics of such composites to determine their full potential as transducers. In this paper, a recently derived model for piezoelectric properties of DEP structured PZT-polymer composites[11] is expanded for high field behavior and compared to experimental results. Additionally, results from resonance measurements are presented and compared to existing theory.

THEORY

The orientation of non-spherical, high-aspect ratio particles in a dielectric fluid will influence the electric field acting on them. Short fiber particles in a continuous matrix can be approximated by treating them as homogeneous ellipsoidal inclusions. The depolarization factor, N, for homogeneous ellipsoid with semi-axes a, b, c in a uniform electric field is given by the following equation:[13]

$$N_i = \frac{abc}{2} \int_0^\infty \frac{ds}{(s+i^2)\beta} \quad (i=a,b,c),$$ (1)

where $\beta^2 = (s+a^2)(s+b^2)(s+c^2)$. For ellipsoids oriented with their long axis, c, parallel to the electric field direction, $i = c$.

Aligned ellipsoidal particles in composites

In the dilute limit, the relative electric field acting on an ellipsoidal inclusion with aspect ratio $AR = c/a \approx l_2/w_2$ (see Figure 1) oriented in the electric field direction, Γ_{AR}, is given by[14]

$$\Gamma_{AR} = \frac{E_{2,dilute}}{E_{app}} = \frac{\varepsilon_1}{\varepsilon_1 + N_z(\varepsilon_2 - \varepsilon_1)},$$ (2)
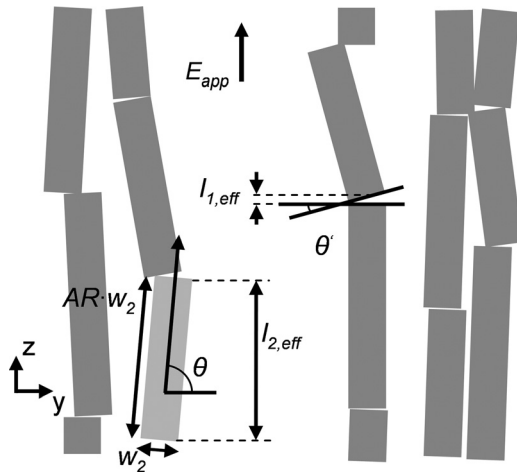

FIG. 1. Schematic of a cross section of the aligned fibers including the particle dimensions, w_2, l_2 ($=AR \cdot w_2$) and orientation angle, θ, and the difference in angle between two fibers, θ', from which the characteristic dimensions $l_{2,eff}$ and $l_{1,eff}$ are derived.

where ε_1 is the permittivity of the matrix and ε_2 is the permittivity of the ellipsoidal inclusion.

When the particles are in close proximity to each other, which is the case in non-dilute dielectrophoretically processed composites, interaction between the particles occurs. By treating the particle and matrix as two capacitors connected in series, the relative electric field acting on the particle, Γ_S, can be described using the size ratio between particle thickness, $l_2 = AR \cdot w_2$, and thickness of the matrix layer in between the particles, l_1, which is defined as $R = \frac{l_2}{l_1}$ and the permittivity of the both phases

$$\Gamma_s = \frac{E_{2,series}}{E_{app}} = \frac{(1+R)\varepsilon_1}{\varepsilon_2 + R\varepsilon_1}.$$ (3)

The combination of the effects described in Eqs. (2) and (3) gives the relation for the relative electric field acting on DEP structured ellipsoidal particles[11]

$$\Gamma_{eff} = \frac{E_2}{E_{app}} = \Gamma_{AR} + (1 - \Gamma_{AR})\Gamma_s$$

$$= 1 - \frac{\left(N_{z,eff}(\varepsilon_1 - \varepsilon_2)^2\right)}{(\varepsilon_2 + R_{eff}\varepsilon_1)\left(\varepsilon_1 + N_{z,eff}(\varepsilon_2 - \varepsilon_1)\right)}.$$ (4)

Here, $N_{z,eff}$ is the effective depolarization factor in the direction of the electric field and $R_{eff} = \frac{l_{1,eff}}{l_{2,eff}}$ is the ratio of effective particle size over effective inter-particle distance. Both these parameters depend on the AR, of the particles and their average orientation, θ (see Ref. 11, for details).

Using the fact that the particle and matrix are connected in series, the (average) electric field acting on the matrix phase in the region between two particles, E'_1, can be calculated

$$\frac{E'_1}{E_{app}} = (1 - \Gamma_{eff})R_{eff} + 1.$$ (5)

Note that the electric field acting on the matrix region between the particles, E'_1 is different than the electric field acting on the matrix region surrounding the particle chains, E_1, which is simply $E_1 = E_{app}$ due to parallel connectivity.

Assuming a non-piezoelectric matrix, the equations for permittivity and piezoelectric charge constants of non-ideally aligned high aspect ratio particle composites are[11]

$$\varepsilon_{DEP} = \varphi\left[\frac{(\Gamma_{eff}\varepsilon_2 - \varepsilon_1)\varepsilon_2}{(\varepsilon_2 - \varepsilon_1)} - (\Gamma_{eff}d_{332})^2 \frac{1-\varphi}{\varphi s_1 + (1-\varphi)s'_{332}}\right]$$
$$+ (1-\varphi)\varepsilon_1,$$ (6)

$$d_{33DEP} = \left[\frac{\varphi s_1}{\varphi s_1 + (1-\varphi)s'_{332}}\right]\Gamma_{eff}d_{332},$$ (7)

where φ is the PZT volume fraction, s_1 and s_{332} are the compliances of the (isotropic) polymer and ceramic inclusions, s'_{332} is the equivalent compliance of the chains of particles,[8]

and d_{332} is the piezoelectric charge constant of the ceramic inclusions.

The high field polarization, P, and strain, S, properties of piezoelectric 1-3 composites with continuous fibers[15] as a function of applied field are

$$P(E_{app}) = \varphi P_2(E_{app}) + [1 - \varphi]P_1(E_{app})$$
$$- \left[\frac{\varphi[1 - \varphi]d_{332}^2(E_{app})E_{app}}{\varphi s_1 + (1 - \varphi)s_{332}^E} \right], \quad (8)$$

$$S(E_{app}) = S_2(E_{app}) \left[\frac{\varphi s_1}{\varphi s_1 + (1 - \varphi)s_{332}^E} \right], \quad (9)$$

where $P_1(E_{app})$, $P_2(E_{app})$, $S_2(E_{app})$, and $d_{332}(E_{app})$ are directly dependent on the applied field E_{app}. Equations (8) and (9) are obtained by multiplying the equations for ε and d_{33} of a 1-3 composite by the applied electric field.[15,16] For DEP structured composites with high AR particle inclusions, the polarization and strain of the particle chains as a function of applied electric field can be calculated using the above equations by replacing $P_2(E_{app})$ with $P_2'(E_{app})$, $S_2(E_{app})$ with $S_2'(E_{app})$, the effective polarization and strain of the aligned particle chains and s_{332} with s_{332}' and d_{332} with d_{332}', the effective compliance and charge constant of the DEP aligned particle chains.[8]

Electromechanical coupling factors of DEP structured composites

From impedance measurements, an estimate of the thickness mode coupling factor, k_t can be made from the thickness resonance if the thickness of the sample is low compared to lateral dimensions.[17] The k_t can be calculated using the following equation:[18]

$$k_t = \left(\frac{\pi f_s}{2 f_p} \tan \left[\frac{\pi}{2} \frac{f_p - f_s}{f_p} \right] \right)^{1/2}, \quad (10)$$

where f_p is the frequency at maximum resistance and f_s is the frequency at maximum conductance.

EXPERIMENTAL

Materials manufacturing

PZT fibers were manufactured by wet spinning a PZT powder (PZT5A4, Morgan Electroceramics, Ruabon, UK) with a Cellulose Acetate binder (Acros Organics). The fibers were sintered at 1200 °C for 1 h in air in a closed Al_2O_3 crucible. PZT fibers were then broken to form high aspect ratio particles, with aspect ratios ranging from 5 to 15. PZT fibers were mixed with a polyurethane (PU, Crystal Clear 202, Smooth-on Inc, Easton, USA) and dielectrophoretically processed during the curing stage of the polymer to form structured composites. The applied structuring electric fields ranged from 0.5 kV/mm to 4 kV/mm to achieve different levels of alignment. Further details of the procedure are described elsewhere.[11] As reference samples, 1-3 composites with continuous fibers were manufactured using the same polyurethane matrix material in addition to bulk PZT ceramics. The bulk ceramic samples and fibers were sintered using the same conditions.

Materials characterization

Low field permittivity of the composites was measured at a fixed frequency of $f = 1$ kHz using an HP 4284A LCR meter. Low field direct d_{33} constants were obtained using a Berlincourt type d_{33} meter (PM3000, PiezoTest, UK). Bipolar polarization of the cured composite samples was measured using a modified Sawyer Tower circuit. The polarization was measured by applying a triangular voltage waveform using a Trek P0621P 30 kV amplifier. The frequency of the applied voltage signal was 1 Hz for the DEP structured composites and 0.1 Hz for the 1-3 composites and PZT ceramics for polarization measurements and 0.1 Hz for all samples for the strain measurements.
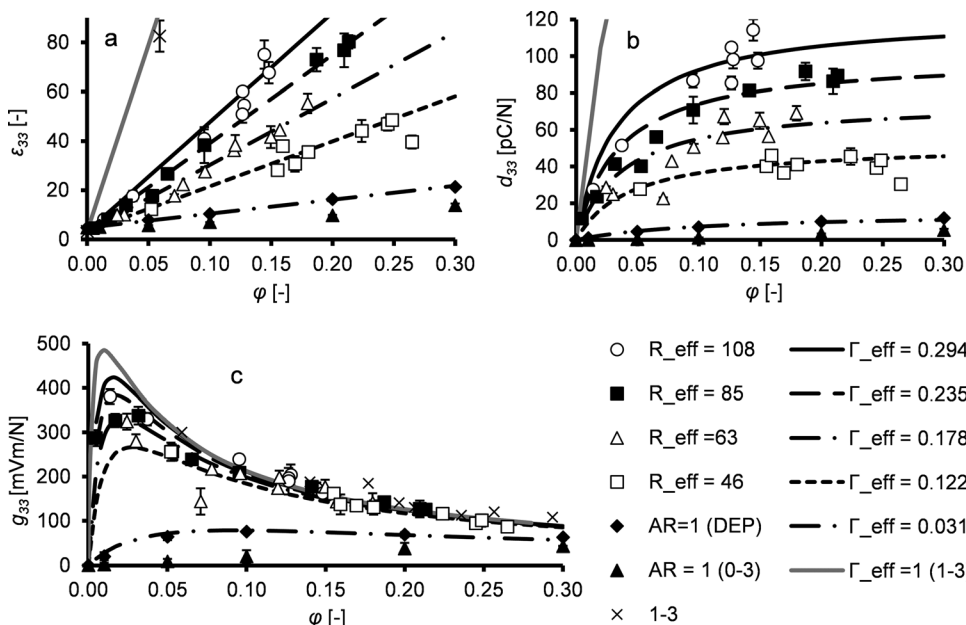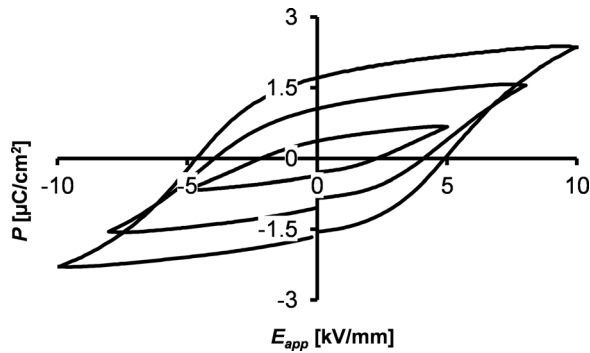

FIG. 2. Relative permittivity (a), piezoelectric charge constants (b), and piezoelectric voltage constants (c) of 1-3 fiber composites and dielectrophoretically aligned composites as a function of particle volume fraction for different R_{eff} compared to model values using Eqs. (6) and (7) for ε and d_{33}, respectively. The values for particle composites ($AR = 1$) were taken from Ref. 8.

FIG. 3. Typical polarization hysteresis loop of a DEP aligned composites. Composite properties are $\varphi = 0.2$ and $R_{eff} = 85$.

Simultaneously, the strain hysteresis was measured using a custom made sample holder fitted with a linear variable differential transformer (LVDT) connected to a lock-in amplifier (Stanford Research SR830). The samples were subsequently poled at 8 kV/mm at 90 °C in a silicone oil bath for 30 min. The poling field was only removed after cooling the samples to room temperature. After poling, unipolar polarization and strain measurements were done using the same setup as for the bipolar measurements. Low field dielectric measurements were performed at 1 kHz using an impedance meter (HP 4284A). Impedance measurements were made using an HP4194a impedance analyzer and a compensated 16334A contact fixture. After piezoelectric characterization, optical micrographs of the composites cross sections were made. These were analyzed to assess the average orientation of the short fibers in the composites (θ). Per sample, 4 micrographs were taken at different depths of the composite and image analysis using the method described in Ref. 8 was used to obtain the average orientation angle of the fibers.

RESULTS

Dielectric and piezoelectric properties at low fields

The dielectric and piezoelectric properties as a function of PZT volume fraction of composites with different R_{eff} are presented in Figure 2. The corresponding curves are modeled using Eqs. (6) and (7) for ε and d_{33}, respectively, using the corresponding values for Γ_{eff}. The relation between R_{eff} and Γ_{eff} is described in detail in Ref. 11. The ε and d_{33} values for these DEP structured composites are higher than traditional 0-3 composites but do not reach the values for low volume fraction 1-3 composites with continuous fibers.[11,15,19] The g_{33} values for the DEP structured composites are, however, comparable to the 1-3 composite values.

Polarization and strain at high electric fields

The typical polarization behavior as a function of electric field of a DEP structured composite is presented in Figure 3. The microstructural properties of this composite were $\varphi = 0.2$, $AR = 11$, $\theta = 68°$, yielding an effective size ratio of $R_{eff} = 85$. In Figure 4, the polarization of two DEP composites with $\varphi = 0.2$, $AR = 11$, $\theta = 68°$, $R_{eff} = 85$ and $\varphi = 0.2$, $AR = 6$, $\theta = 49°$, $R_{eff} = 45$, is compared to that of a comparable 1-3 composite with continuous fibers and bulk PZT5A4 ceramic. The polarization as a function of applied electric field of DEP structured composites is similar in form to the bulk PZT5 hysteresis but with much higher coercive fields compared to bulk PZT and 1-3 PZT-polymer composites. Typical coercive fields of around 4-6 kV/mm were found for the aligned short fiber composites at an applied field of $E_{app} = 10$ kV/mm, depending on the aspect ratio and average orientation angles of the fibers in the composite.

The bipolar strain hysteresis as a function of applied field is presented in Figure 5. The shape of the strain loops of the DEP aligned composite materials is slightly asymmetrical. At
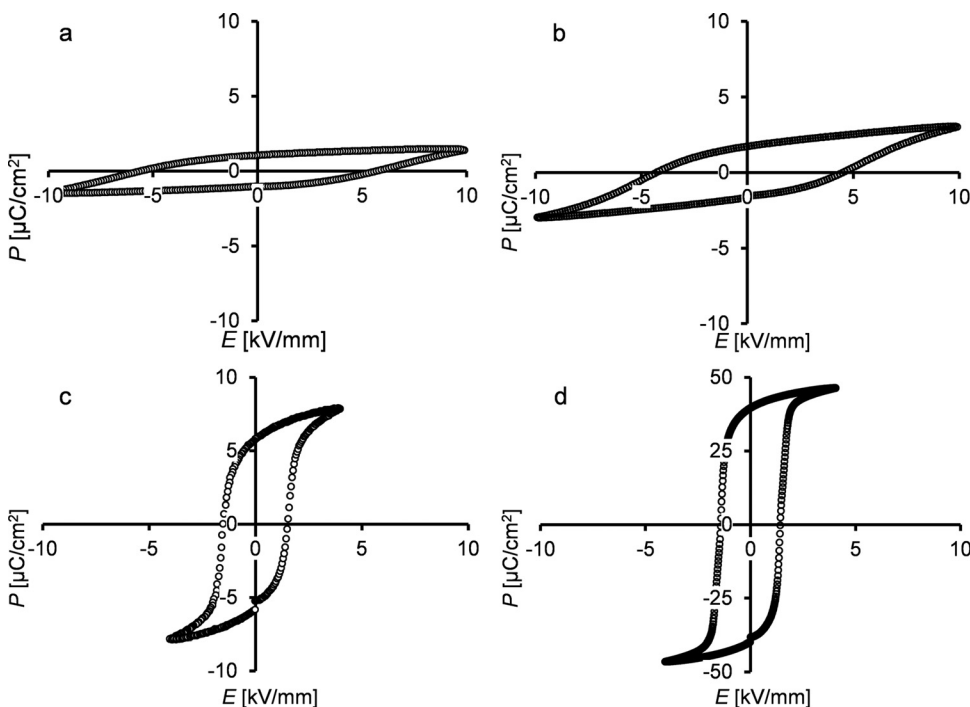

FIG. 4. Comparison between a DEP aligned fiber composites ($\varphi = 0.2$, $R_{eff} = 45$) and ($\varphi = 0.2$, $R_{eff} = 85$), 1-3 fiber composite ($\varphi = 0.2$), and PZT 5A4 bulk ceramic.
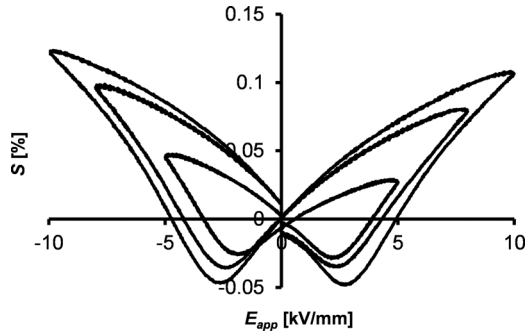
FIG. 5. Typical evolution of bipolar strain hysteresis loop of a DEP structured composite ($\varphi = 0.2$, $R_{eff} = 85$).

low fields, this effect is most visible. The strain response is comparable to the response of 1-3 composite and bulk PZT materials (Figure 6). The coercive field for the DEP structured composites is higher while the maximum strain of the composite is lower than that of the 1-3 composite and that of the bulk material.

The unipolar polarization (Figure 7) and strain hysteresis (Figure 8) in the positive poling direction were measured for poled composites and the corresponding values for ε_{33} and d_{33} were calculated by $\varepsilon_0 \varepsilon_r(E) = \frac{dP}{dE}$, and $d_{33}(E) = \frac{dS}{dE}$. Both ε_{33} and d_{33} increase with applied field up to a maximum, after which the values decrease for all systems. The position of this maximum is different for the different materials. The PZT ceramic reaches its maximum at around $E_{app} = 1\,kV/mm$ while for the composites, the maximum is reached at a higher applied field.

Impedance measurements around resonance

Impedance measurement results are presented in Figure 9. The half wave thickness resonance characteristics are shown for a PZT5A4 disk and 1-3 composite ($\varphi = 0.24$) and

two different DEP structured composites. The DEP structured composites contain inclusions with different average aspect ratios, a "high AR" sample ($\varphi = 0.15$, $AR_{eff} = 11$, $R_{eff} = 116$) and "low AR" sample ($\varphi = 0.24$, $AR_{eff} = 6$, $R_{eff} = 41$). The range of the resonance frequencies that were measured lie between 1 and 7 MHz and depend on sample geometry and material properties.

DISCUSSION

Electric field distributions in the composites

Using Eq. (4), the effects of aspect ratio and particle length/inter-particle matrix thickness ratio on the normalized electric field acting on an ellipsoidal PZT particle for a fixed relative permittivity values of $\varepsilon_1 = 3.2$ and $\varepsilon_2 = 1550$ are given in Figure 10. These permittivity values are low-field permittivity values of the PU matrix and PZT fibers, respectively.[11]

As follows from Eq. (5), the electric field values are greatest in the matrix region between the fibers. The analytical results for fixed relative permittivity values of $\varepsilon_1 = 3.2$ and $\varepsilon_2 = 1550$ are presented in Figure 11.

The results in Figures 10 and 11 show that the electric field acting on the particle increases when the aspect ratio of the particles increases and when the inter-particle distance decreases. However, for small aspect ratio particles, the concentration in electric field between 2 closely connected particles increases dramatically. The results from Eq. (5) indicate that electric fields between closely spaced filler particles can be orders of magnitude higher than the applied field. If the aspect ratio of the filler particles is high enough, however, the peak electric field between the particles drops. The results in Figure 11 are consistent with reports that breakdown electric fields are lower in the direction of alignment for DEP aligned composites with low *AR* particles
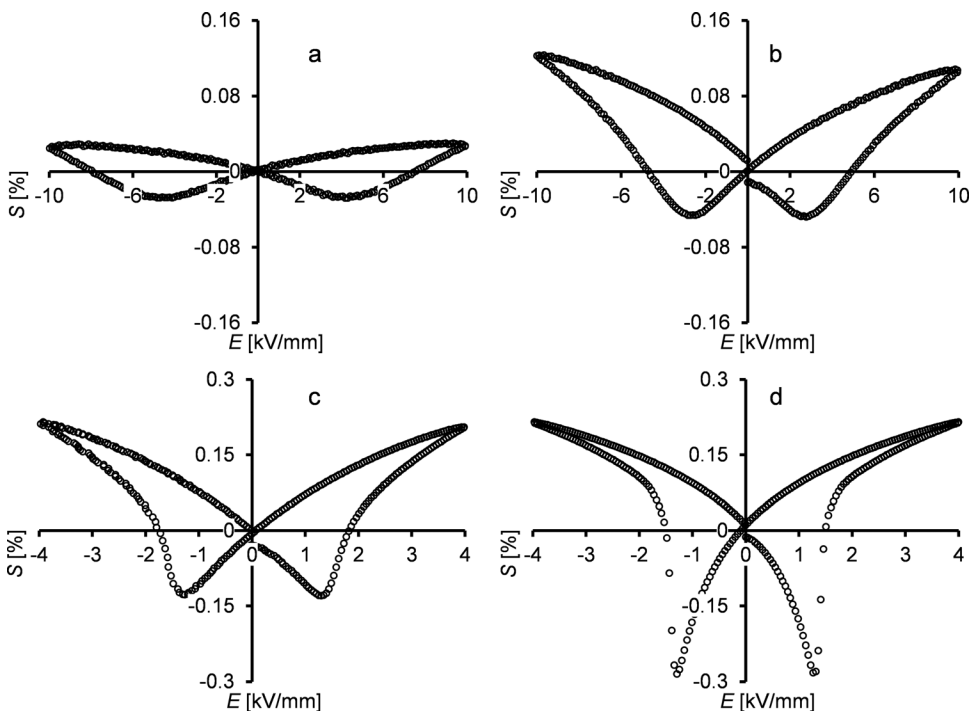

FIG. 6. Comparison between a DEP aligned fiber composites ((a) $\varphi = 0.2$, $R_{eff} = 45$) and ((b) $\varphi = 0.2$, $R_{eff} = 85$), 1-3 fiber composite ((c) $\varphi = 0.2$), and PZT 5A4 bulk ceramic (d). Note the scale difference in x-, and y-axes for (a) and (b) compared to (c) and (d).
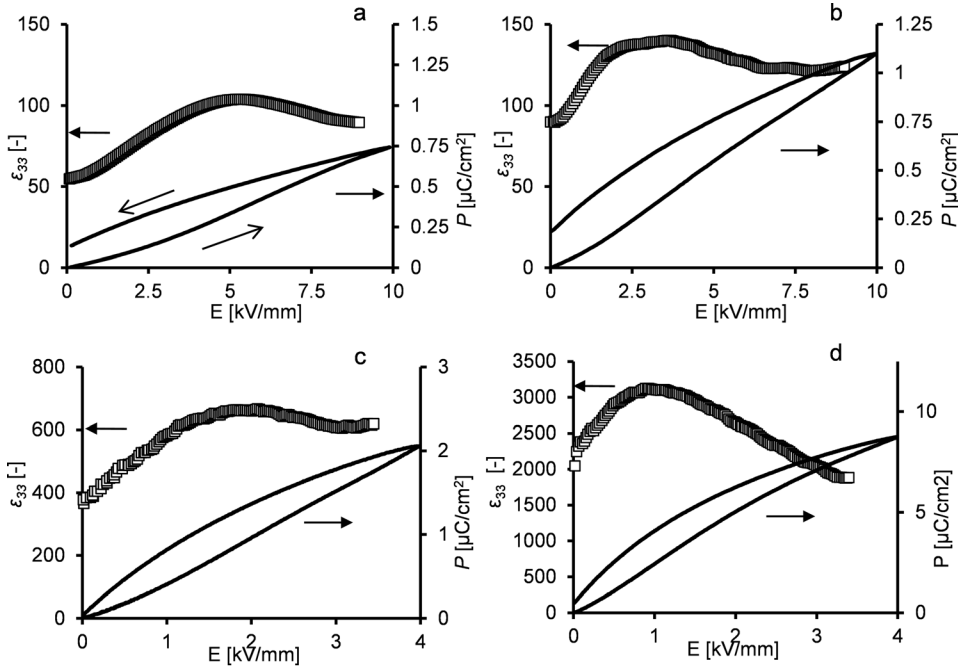
FIG. 7. Unipolar polarization hysteresis of DEP structured composites ((a) $\varphi = 0.2$, $R_{eff} = 45$) and ((b) $\varphi = 0.2$, $R_{eff} = 85$), 1-3 fiber composite ((c) $\varphi = 0.2$), and PZT 5A4 bulk ceramic (d) and associated values of the relative permittivity, ε_{33}. In (a), the open arrows indicate the direction of applied field.

compared to composites with x-y aligned or randomly dispersed particles[20–22] and may be interesting for nanowire based composite capacitors.[9]

High field properties of PZT-PU composites

The polarization of the DEP structured quasi 1-3 composites is always lower than the polarization of the 1-3 composites and bulk ceramics at the same applied electric field. This lower polarization can be expected from the analysis in "Electrical field distributions in the composites" section. Using Eqs. (8) and (9), the polarization and strain of the DEP aligned chains of PZT particles can be extracted. These values can be regarded as an upper bound for the DEP structured composites with a corresponding R_{eff}. The extracted values are presented in Figure 12. The maximum achieved strain of 0.15% for $R_{eff} = 85$ is (Figure 8) is comparable to PZT ceramics operated at $E_{app} = 2.5$ kV/mm. In practice, this electric field level is often taken as an operational limit of applied field to ensure adequate lifetime of the ceramics. The fatigue characteristics of the DEP structured composites operated at $E_{app} = 10$ kV/mm have not been tested, but if a polymer with sufficiently high electrical strength is used as a matrix, the practical operation strain limit can be made comparable to that of PZT. However, the importance of the R_{eff} value is illustrated in Figure 12 when comparing the composite with $R_{eff} = 85$ to the composite with $R_{eff} = 45$, which does not achieve one third of its maximum strain. The electric field ratio acting on the particles determines the achievable strain for a fixed applied field. The electric field ratio is
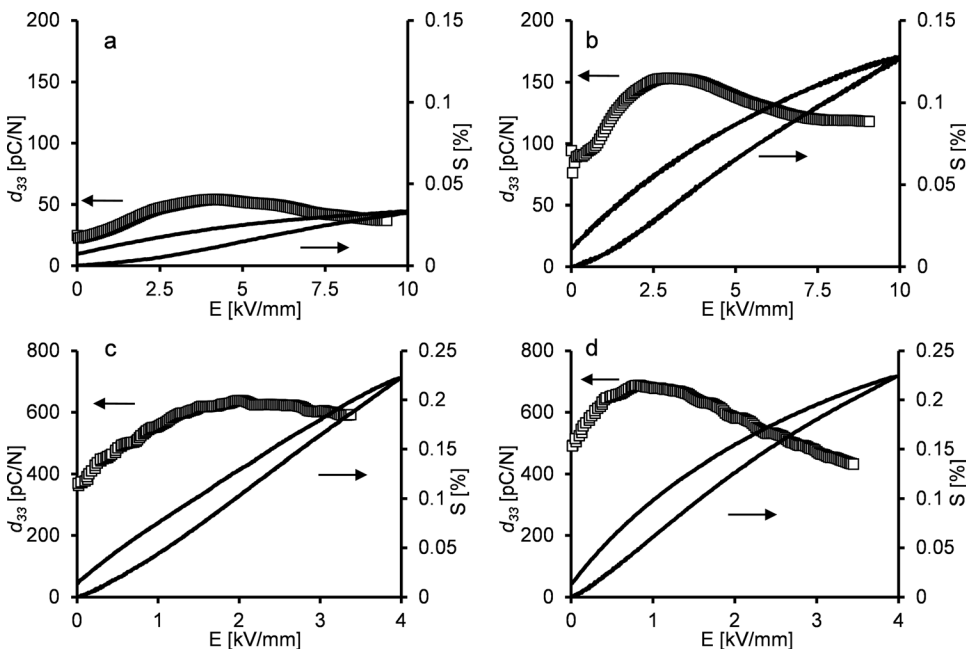

FIG. 8. Unipolar strain hysteresis of DEP structured composites ((a) $\varphi = 0.2$, $R_{eff} = 45$) and ((b) $\varphi = 0.2$, $R_{eff} = 85$), 1-3 fiber composite ((c) $\varphi = 0.2$) and PZT 5A4 bulk ceramic (d) and associated d_{33} values.
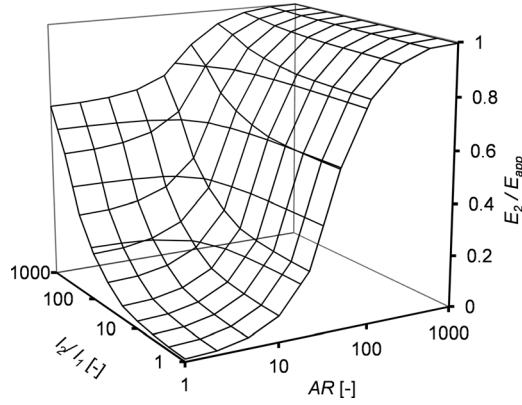
FIG. 9. Impedance magnitude and phase around resonance of DEP structured composites ((a) $\varphi = 0.24$, $R_{eff} = 41$) and ((b) $\varphi = 0.15$, $R_{eff} = 116$), 1-3 fiber composite ((c) $\varphi = 0.24$) and PZT 5A4 bulk ceramic disk (d). The KLM fits for each sample are represented by the solid (magnitude) and dashed (phase) lines.

FIG. 10. Electric field ratio acting on an ellipsoidal PZT particle as a function of aspect ratio, AR and different particle spacing, R using Eq. (4).

retained at high fields resulting in an increase in ε_{33} and d_{33} of the composites. Both ε_{33} and d_{33} exhibit a maximum in the DEP aligned composites. This result indicates that the value of Γ_{eff} may change at high fields. The position of the maximum is different for composite with a different value of R_{eff}, shifting to a lower E_{app} for higher R_{eff}. No signs of breakdown were observed in the composites at $E_{app} = 10\,\text{kV}/$ mm over the whole range of R_{eff} that was tested. This effect may be because the composites with a higher R_{eff} all tended to have higher AR particles. A higher AR decreases E_1, avoiding breakdown (see Eq. (5) and Figure 11).

The difference in maximum polarization between bulk PZT5A4 ceramics (see Figure 7) and the fiber properties (Figure 12) derived from composite materials is in part related to the clamping effect caused by the matrix in the low volume fraction composites.[15,23] Therefore, it must be
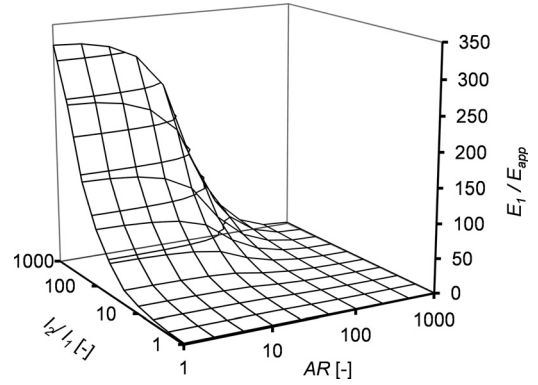
noted that the fiber properties presented here are the effective fiber properties in the composite at a volume fraction of $\varphi = 0.2$ and single fiber properties will differ.[23] This volume fraction is comparable to the volume fractions of the DEP structured composites. The measured coercive field of unconstrained PZT fibers will also be slightly higher than the coercive field of the low φ 1-3 composite due to clamping.[24] The DEP structured composites show higher coercive and saturation electric fields than the 1-3 composites. In general, $\frac{dP}{dE}$ is smaller for the DEP aligned composites and is a result of $\Gamma_{eff} < 1$ (see Eq. (4)). The coercive field of the composites is also related to Γ_{eff} and results in $E_{c\,DEP} > E_{c1-3}$. The maximum strain (Figure 6) in the positive poling direction of the 1-3 composites is higher than that of the bulk ceramic and relatively high compared to values reported in literature.[15,25] This is attributed to the uniaxial strain state in the fibers, which have relatively high aspect ratio and small lateral dimensions, especially for the continuous 1-3 fiber composites. This effect was also previously reported for small
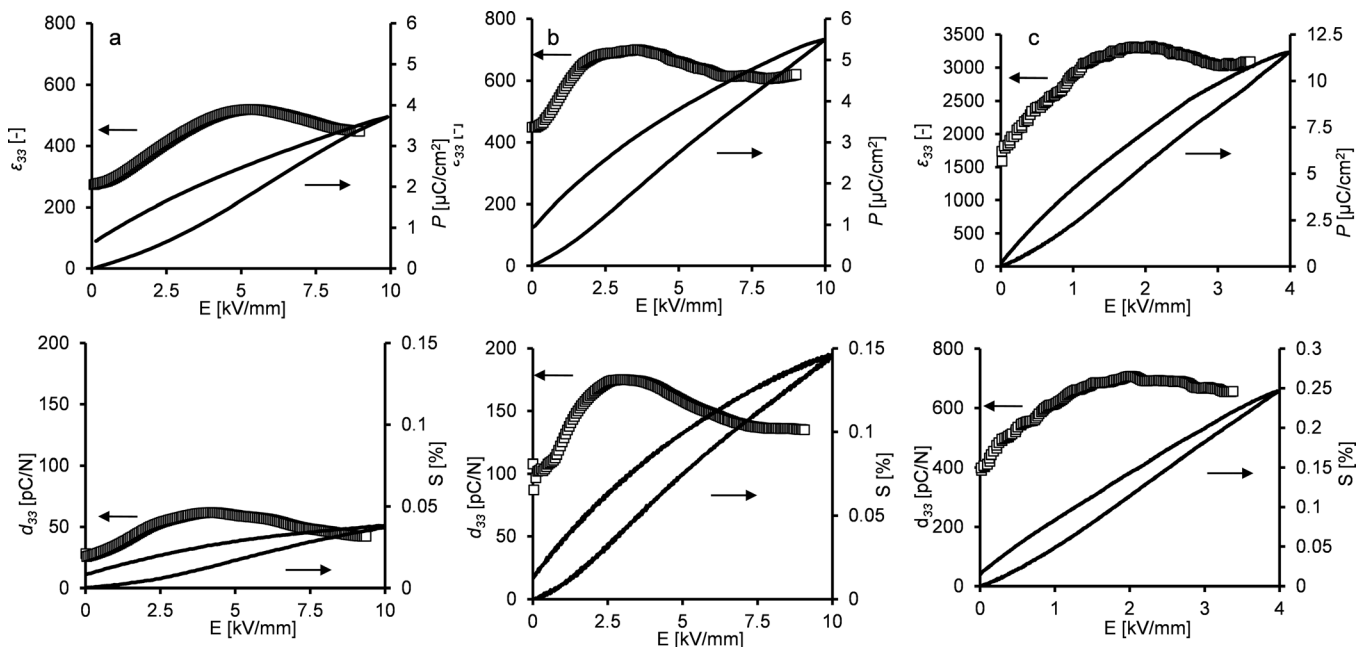

FIG. 11. The effective electric field concentration in the matrix layer between two adjacent particles as a function of particle dimensions and inter-particle distance.
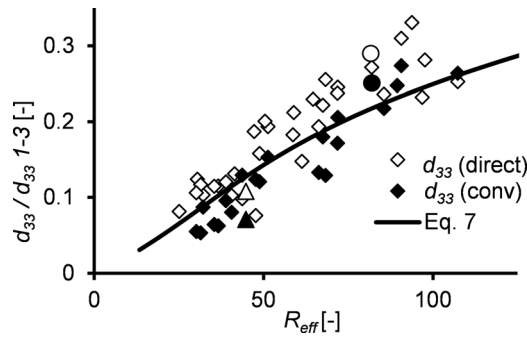
FIG. 12. Unipolar polarization and strain hysteresis of DEP structured composites ((a) $R_{eff} = 45$) and ((b) $R_{eff} = 85$) and 1-3 fiber composite (c) and associated ε_{33} and d_{33} values. The polarization and strain values were normalized for the PZT phase in the composites using Eqs. (8) and (9). The bulk PZT values can be found in Figures 8(d) for comparison.

diameter fibers[15] because the stress transfer from fiber to matrix depends on the fiber surface area.[26] Alternatively, a relatively low maximum compressive strain at the point of polarization reversal is seen for 1-3 composites and DEP structured composites. This is again caused by clamping of the high aspect ratio fibers,[15] since depolarization of PZT is known to be aided by compressive stress[27] leading to lower compressive strains at polarization reversal.[23,24] In the DEP structured composites, an even smoother strain reversal behavior is seen due to the distribution of fiber aspect ratios and orientations. When the polarization of each particle in the composite is oriented in the same direction, the contributions are averaged. But when the polarization is switched this difference becomes more visible. In the region close to the coercive field of the composite, the polarization of some of the particle inclusions will be switched while others are still polarized in the poling direction. The DEP structured composites all exhibited asymmetric strain polarization behavior as the example in Figure 5. No clear virgin polarisation curve could be measured for any of the DEP aligned composites, suggesting (partial) poling during manufacturing.

In the cured DEP aligned composites, the electric field in the matrix region between two adjacent particles is dramatically increased because the particles are brought in close proximity of each other by the DEP force. The permittivity increases as a function of the field component in the matrix phase, E_1'. This component is a function of the particle dimension and inter-particle distance as can be seen in Figure 11. The electric field intensities for sample composites can be estimated based on the low field values using Eq. (5). They are on the order of $50 < E_1'/E_{app} < 115$ if the permittivity of the PU phase is kept constant at $\varepsilon_1 = 3.2$ and no loss is considered (see Figure 11). This would yield electric fields of up to $E_1' = 1000 \, \text{kV/mm}$ at $E_{app} = 10 \, \text{kV/mm}$. This is about 50 times the typical breakdown field of bulk polyurethane. However, no breakdown is observed in the composites during these measurements. The breakdown field of nano-scale interfaces is known to be much higher than breakdown field of bulk material,[20] which might partly explain why the composite samples do not break down at these applied voltages. If the composite features can be scaled down, f.i. using nanowires as particle inclusions[28,29] the fea-

ture size will decrease. This will be beneficial in two ways. The total applied voltage will decrease and the inter particle distance will decrease for constant R_{eff}. This effect will result in an even thinner inter-particle matrix layer with a higher dielectric breakdown electric field.[20]

In Figure 13, the converse d_{33} of the composites is compared to the direct piezoelectric measurements, which were measured on a Berlincourt d_{33} meter (i.e., the values in Figure 2(b)). The DEP structured composite d_{33} values relative to 1-3 composite d_{33} values of the same volume fraction are plotted, along with the theoretical values calculated using Eq. (7). The values are comparable, though the converse measurement yields slightly lower values than the direct measurement. The maximum converse d_{33} is compared to the low-field converse effect in Figure 14. The high field d_{33} data are compared to the calculated d_{33} of 1-3 composites at the corresponding electric field using $E_2 = \Gamma_{eff} E_{app}$, where the low field value for Γ_{eff} was used as an approximation for the applied field ratio on the particle inclusions. The relative d_{33} at high fields is slightly higher than the low field ratio for composites, suggesting a modest increase of Γ_{eff} at higher applied fields.

In general, DEP structured PZT-polymer composites with high aspect ratio particle inclusions have low field piezoelectric constants which are much higher than those of traditional 0-3 granular particle composites and have piezoelectric voltage constants which are comparable to 1-3 composites (see Figure 2). This high g_{33} is beneficial when the material is used as a transducer receiver. At high applied electric fields, the d_{33} increases towards a maximum at around 2.5-5 kV/mm and subsequently decreases slightly. Because of its higher maximum applied field, the electromechanical strain that can be achieved is closer to the ceramic and 1-3 composite values than the d_{33} values alone would suggest.

Thickness coupling factors of DEP structured composites

Using the data of the impedance plots for frequencies around the resonance frequency for three composites and one reference bulk PZT sample (Figure 9), the thickness coupling factors were calculated using Eq. (10). It is known that for highly damped systems the use of Eq. (10) may lead to inaccuracies in the calculated k_t values.[30] Therefore, a
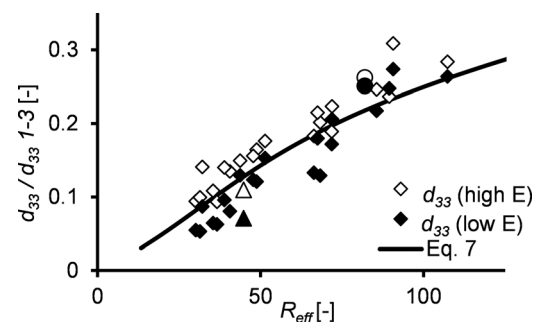

FIG. 13. Converse d_{33} at field low conditions ($E_{app} = 0.1 \, \text{kV/mm}$), compared to the direct d_{33}. The triangles are values for the example composite with $R_{eff} = 45$ and circles are values for the composite with $R_{eff} = 85$.
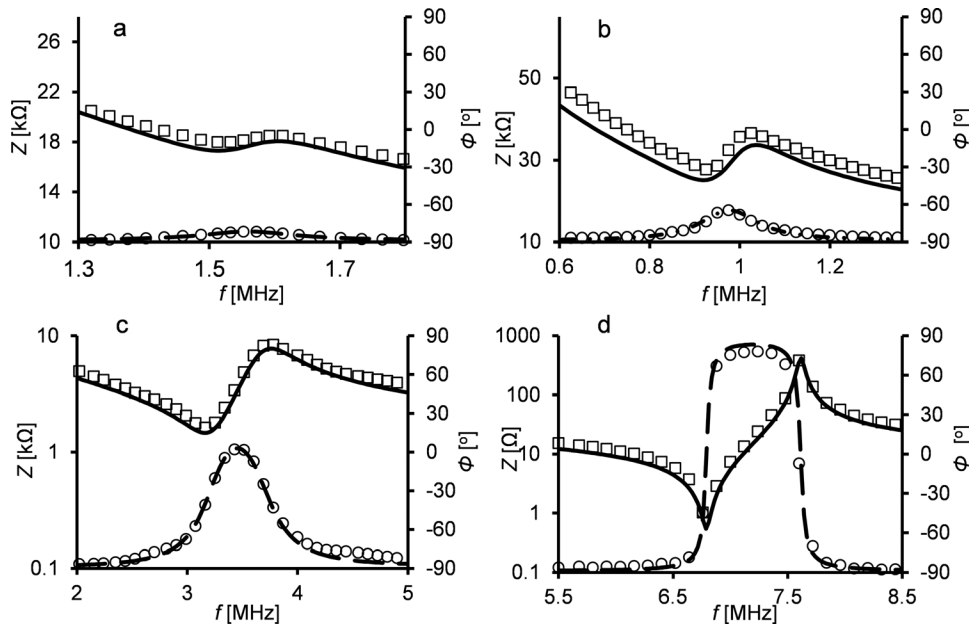
FIG. 14. Maximum d_{33} at high field conditions compared to the d_{33} under low field conditions (converse effect). The triangles are values for the example composite with $R_{eff} = 45$ and circles are values for the composite with $R_{eff} = 85$.

comparison to the calculated coupling factors was made by fitting a custom implementation of the KLM (Krimholtz, Leedom, Matthaei) equivalent circuit model[31,32] to the impedance data for k_t. The mechanical quality factor, Q_m, was separately estimated using the technique outlined in Ref. 33. The fitted impedance curves are presented Figure 9. In Table I, calculated k_t values using Eq. (10) and the fitted k_t values are compared. The values calculated using Eq. (10) slightly underestimate k_t compared to the fitted values from the equivalent circuit models.

The "low AR" DEP structured composites show a thickness coupling factor which is comparable to that of PVDF polymer and "high AR" DEP materials are comparable to PVDF-TrFE polymers. The extremely low Q_m of the DEP structured composites are possibly the result of the size distribution of the inclusions, causing local variations in stiffness and piezoelectric coefficients within the material. These local differences generally broaden the resonance peak of the sample.[34] This effect has been reported for unstructured piezoelectric PZT-polymer composites with high PZT volume fractions.[35] In the 1-3 composite, the same effects are caused by local variations in fiber packing density due to the processing technique used (see experimental section). Thus, resonance measurements show that the DEP aligned composites posses a fair amount of electromechanical coupling for such low volume fractions of PZT and bandwidth is high due to mechanical damping. The high coupling

factors are consistent with the high d_{33} values that were measured for the composites at low frequency. Also, electrical loss remains relatively low (tan $\delta_e \approx 0.02 - 0.04$ in MHz frequency range). These electrical losses are much lower than for PVDF (tan $\delta_e \approx 0.24$ in the MHz range).[36] Also the lower frequency constant (see Table I) allows for thinner transducers compared to PZT devices. Therefore, the DEP composites could potentially be an interesting alternative for transducers which are now using piezoelectric polymers. These properties could make the composites interesting candidates for large area transducers. They are especially interesting if integration with existing complex shaped structures is needed and a large shaping freedom is required.[2,12] Analogous to continuous PZT fiber composites,[37] DEP structured composites can also be employed in-plane by making use of interdigitated electrodes.[38] This electrode structure creates the possibility to manufacture thin and compliant piezoelectric transducer coatings with higher coupling factors at lower PZT volume fractions than conventional 0-3 composite coatings based on randomly dispersed particles such as mentioned in Ref. 2.

CONCLUSIONS

DEP structured PZT-polymer composites with high aspect ratio particle inclusions have low field piezoelectric constants which are much higher than those of traditional 0-3 granular particle composites, especially at low volume fractions. They can achieve piezoelectric voltage constants which are comparable to 1-3 composites with continuous fibers. This high g_{33} is beneficial when the material is used as a transducer receiver. Also significant electromechanical coupling at high frequencies was measured at resonance for DEP structured composites. Polarization, strain, and coercive field of the fibers were all found to be dependent on R_{eff}, the effective length of the fiber over the distance between the fibers. The electric field corresponding to a maximum of ε_{33} and d_{33} is dependent on R_{eff}, shifting to a lower E_{app} for higher R_{eff}. Polarization, strain, and coercive field of the

TABLE I. Calculated and fitted thickness coupling factor (k_t) and mechanical quality factor (Q_m) and calculated thickness frequency constant (N_3^D) for the DEP aligned composites, 1-3 composite, and PZT5A disk.

Material	k_t (Eq. (10))	k_t KLM fit[31]	Q_m[33]	Q_m KLM fit[31]	N_3^D [m/s]
Low AR, DEP composite	0.10	0.13	6.7	8.9	1100
High AR DEP composite	0.26	0.28	5.9	6.5	1220
1-3 Composite	0.47	0.52	6.5	8.2	1390
PZT5A4 disk	0.49	0.49	123	133	2030

fibers are found to depend on R_{eff}. For composites with well aligned high aspect ratio particles ($R_{\text{eff}} \sim 85$), the electromechanical strain that can be achieved approaches the values for the ceramic and 1-3 fibrous composites. The observed dependences can be explained by a model taking into account the spatial arrangement of the particles and the material properties. If the thickness can be scaled down while retaining the high aspect ratio of the inclusions, for instance, by using PZT nanowires as the high aspect ratio particles, this type of composite can possibly be employed for transducers which are cost effective and relatively simple to process. These materials are especially interesting if integration with existing structures is needed, because the composites can be processed at low temperatures.

ACKNOWLEDGMENTS

[1]R. E. Newnham, D. P. Skinner, and L. E. Cross, Mater. Res. Bull. **13**, 525 (1978).

[2]S. Egusa and N. Iwasawa, J. Mater. Sci. **28**, 1667–1672 (1993).

[3]C. J. Dias and D. K. Das Gupta, IEEE Trans. Electr. Insul. **3**, 706 (1996).

[4]R. E. Newnham, A. Safari, G. Sa-Gong, and J. Giniewicz, in *IEEE International Ultrasonics Symposium* (1984), p. 501.

[5]H. A. Pohl, *Dielectrophoresis: The Behavior of Neutral Matter in Nonuniform Electric Fields* (Cambridge University Press, Cambridge, 1978).

[6]C. A. Randall, S. Miyazaki, K. L. More, A. S. Bhalla, and R. E. Newnham, Mater. Lett. **15**, 26–30 (1992).

[7]C. P. Bowen, R. E. Newnham, and C. A. Randall, J. Mater. Res. **13**, 205 (1998).

[8]D. A. van den Ende, B. F. Bory, W. A. Groen, and S. van der Zwaag, J. Appl. Phys. **107**, 024107 (2010).

[9]H. Tang, Y. Lin, and H. A. Sodano, Adv. Energy Mater. **2**, 469 (2012).

[10]H. Tang, Y. Lin, C. Andrews, and H. A. Sodano, Nanotechnology **22**, 015702 (2011).

[11]D. A. van den Ende, S. E. van Kempen, X. Wu, W. A. Groen, C. A. Randall, and S. van der Zwaag, J. Appl. Phys. **111**, 124107 (2012).

[12]J. Feenstra and H. A. Sodano, J. Appl. Phys. **103**, 124108 (2008).

[13]C. J. F. Böttcher, O. C. van Belle, P. Bordewijk, and A. Rip, *Theory of Electric Polarization* (Elsevier Scientific, 1978).

[14]A. Sihvola, *Electromagnetic Mixing Rules and Applications* (The Institution of Electrical Engineers, London, UK, 1999).

[15]L. J. Nelson, C. R. Bowen, R. Stevens, M. Cain, and M. Stewart, Proc. SPIE **5053**, 544 (2003).

[16]H. L. W. Chan and J. Unsworth, IEEE Trans. Ultrason. Ferroelectr. Freq. Control **36**, 434 (1989).

[17]M. Kim, J. Kim, and W. Cao, Appl. Phys. Lett. **87**, 132901 (2005).

[18]A. Meitzler, D. Berlincourt, G. Coquin, F. Welsh, H. Tiersten, and A. Warner, *IEEE Standards on Piezoelectricity, ANSI/IEEE Std 176-1978* (The Institute of Electrical and Electronics Engineers, 1987).

[19]H. P. Savakus, K. A. Klicker, and R. E. Newnham, Mater. Res. Bull. **16**, 677 (1981).

[20]V. Tomer and C. A. Randall, J. Appl. Phys. **104**, 074106 (2008).

[21]V. Tomer, C. A. Randall, G. Polizos, J. Kostelnick, and E. Manias, J. Appl. Phys. **103**, 034115 (2008).

[22]J. E. Martin, C. P. Tigges, R. A. Anderson, and J. Odinek, Phys. Rev. B **60**, 7127 (1999).

[23]A. Belloli, J. Heiber, F. Clemens, and P. Ermanni, J. Intell. Mater. Syst. Struct. **20**, 355 (2009).

[24]D. Zhou, M. Kamlah, and D. Munz, J. Eur. Ceram. Soc. **25**, 425–432 (2005).

[25]C. R. Bowen, R. Stevens, L. J. Nelson, A C. Dent, G. Dolman, B. Su, T. W. Button, M. G. Cain, and M. Stewart, Smart Mater. Struct. **15**, 295 (2006).

[26]Q. M. Zhang, W. Cao, H. Wang, and L. E. Cross, J. Appl. Phys. **73**, 1403 (1993).

[27]T. Fett and D. Muntz, Adv. Eng. Mater. **5**, 718 (2003).

[28]H. Tang, Y. Lin, and H. A. Sodano, Proc. SPIE **7978**, 79780S (2011).

[29]C. Andrews, Y. Lin, H. Tang, and H. A. Sodano, J. Int. Mater. Syst. Struct. **22**, 1879 (2011).

[30]F. S. Foster, L. K. Ryan, and D. H. Turnbull, IEEE Trans. Ultrason. Ferroelectr. Freq. Control **38**, 446 (1991).

[31]R. Krimholtz, D. A. Leedom, and G. L. Matthaei, Electron. Lett. **6**, 398–399 (1970).

[32]E. J. W. Merks, J. M. G. Borsboom, M. M. Voormolen, N. Bom, A. F. W. van der Steen, and N. de Jong, Ultrasonics **44**, e705–e710 (2006).

[33]L. N. Bui, H. J. Shaw, and L. T. Zitelli, IEEE Trans. Son. Ultrason. **24**, 331–336 (1977).

[34]M. P. Wenger, P. Blanas, C. J. Dias, R. J. Shuford, and D. K. Dasgupta, Ferroelectrics **187**, 75–86 (1996).

[35]C. Dias, D. K. Das-Gupta, Y. Hinton, and R. J. Shuford, Sens. Actuators, A **37–38**, 343–347 (1993).

[36]F. S. Foster, K. A. Harasiewicz, and M. D. Sherar, IEEE Trans. Ultrason. Ferroelectr. Freq. Control **47**, 1363 (2000).

[37]A. A. Bent and N. W. Hagood, J. Int. Mater. Syst. Struct. **8**, 903 (1997).

[38]D. A. van den Ende, H. J. van de Wiel, W. A. Groen, and S. van der Zwaag, Smart Mater. Struct. **21**, 015011 (2012).